

RELATION BETWEEN SHAPES OF POST-SYNAPTIC POTENTIALS AND CHANGES IN FIRING PROBABILITY OF CAT MOTONEURONES

BY E. E. FETZ* AND B. GUSTAFSSON

From the Department of Physiology, University of Göteborg, Göteborg, Sweden

(Received 25 August 1982)

SUMMARY

1. The shapes of post-synaptic potentials (p.s.p.s) in cat motoneurones were compared with the time course of changes in firing probability during repetitive firing. Excitatory and inhibitory post-synaptic potentials (e.p.s.p.s and i.p.s.p.s) were evoked by electrical stimulation of peripheral nerve filaments. With the motoneurone quiescent, the shape of each p.s.p. was obtained by compiling post-stimulus averages of the membrane potential. Depolarizing current was then injected to evoke repetitive firing, and the post-stimulus time histogram of motoneurone spikes was obtained; this histogram reveals the primary features (peak and/or trough) of the cross-correlogram between stimulus and spike trains. The time course of the correlogram features produced by each p.s.p. was compared with the p.s.p. shape and its temporal derivative.

2. E.p.s.p.s of different sizes (0.15–3.1 mV, mean 0.75 mV) and shapes were investigated. The primary correlogram peak began, on the average, 0.48 msec after onset of the e.p.s.p., and reached a maximum 0.29 msec before the summit of the e.p.s.p.; in many cases the correlogram peak was followed by a trough, in which firing rate fell below base-line rate. The height of the correlogram peak with respect to base-line firing rate increased in proportion to both the amplitude of the e.p.s.p.s and the magnitude of their rising slope (in these data, amplitude and rising slope also covaried).

3. The mean half-width of the correlogram peaks (0.65 ± 0.28 msec (s.d.)) agreed better with the average half-width of the e.p.s.p. derivatives (0.55 ± 0.33 msec) than with the half-width of the e.p.s.p.s (4.31 ± 1.50 msec). The shape of the primary correlogram peak produced by simple e.p.s.p.s often resembled the temporal derivative of the e.p.s.p. rise. For larger e.p.s.p.s, the shape of the correlogram peak closely matched the e.p.s.p. derivative, while smaller e.p.s.p.s in appreciable synaptic noise often generated correlogram peaks somewhat wider than their derivatives. On the other hand, the match between the correlogram trough that followed the peak and the negative slope of the e.p.s.p. was better for the small e.p.s.p.s than for the large e.p.s.p.s; for large e.p.s.p.s the drop in firing rate during the trough was typically limited at zero. These relations were tested further by comparing the integral of the correlogram with the time course of the e.p.s.p. For large e.p.s.p.s, the correlogram

* Present address: Regional Primate Research Center and Department of Physiology and Biophysics, University of Washington, Seattle, WA 98195, U.S.A.

integral matched the rising phase of the e.p.s.p. quite well, although it underestimated the rate of decline of the e.p.s.p.

4. Complex e.p.s.p.s with distinct components during their rising phase often produced correlogram peaks that did not accurately reflect the features in their temporal derivative. Temporal summation of large e.p.s.p.s and summation of their derivatives was linear, but the resulting correlogram peaks did not add linearly; the second correlogram peak was often smaller than the first. However, when small e.p.s.p.s were summed, the correlogram peaks more closely matched the e.p.s.p. derivatives.

5. Compound i.p.s.p.s produced primary correlogram troughs followed by a shallow compensatory peak. The width of the trough extended through the peak of the i.p.s.p., well into the falling phase of the i.p.s.p. During the trough the firing rate usually dropped to zero. Thus, the primary correlogram features produced by large i.p.s.p.s did not resemble any linear combination of the shape of the i.p.s.p. and/or its temporal derivative. Moreover, the integral of the correlogram did not resemble the i.p.s.p.

6. The major observations are consistent with a motoneurone model in which a membrane potential ramp approaches a voltage threshold for spike initiation. Near threshold, e.p.s.p.s superimposed on the ramp advance the occurrence of spikes to their rising phase, producing a correlogram peak resembling their temporal derivative. Synaptic noise would increase the probability of sampling the peak of the e.p.s.p., leading to wider correlogram peaks. I.p.s.p.s would delay the occurrence of spikes to their falling phase.

INTRODUCTION

Synaptically mediated interactions between neurones have been investigated in two types of recording situations. Intracellular recording of post-synaptic potentials (p.s.p.s) evoked by activation of presynaptic cells has revealed synaptic connectivity in terms of excitatory and inhibitory post-synaptic potentials (e.p.s.p.s and i.p.s.p.s). The considerable range of shapes and sizes of p.s.p.s has suggested corresponding differences in the effectiveness of underlying synaptic connexions. Alternatively, extracellular recording has shown that the changes in firing probability of the post-synaptic cell can be used to document its synaptic input from presynaptic cells. In this case the interaction between neurones can be detected by cross-correlating the input events (stimulus or spike trains) with the output spike train of the post-synaptic cell. Certain features of the cross-correlograms have been used to infer the types of underlying synaptic connexions, as previously described (Moore, Perkel & Segundo, 1966; Moore, Segundo, Perkel & Levitan, 1970; Bryant, Marcos & Segundo, 1973; Knox & Poppele, 1977; Kirkwood, 1979). The 'primary effect' of a synaptic interaction is the peak and/or trough nearest the origin of the cross-correlogram; its size and shape normally depend more on the synaptic potentials produced by the connexion than on the firing characteristics of the relevant cells. 'Secondary effects' are the correlogram features farther from the origin, which reflect periodicities in the firing of pre- and post-synaptic cells; they can be used in conjunction with autocorrelograms to infer the direction of the neural interactions (Moore *et al.* 1970).

The relation between the shapes of primary cross-correlogram features and the underlying p.s.p.s is of some consequence. If one knew this transform, one could infer the effects produced by observed p.s.p.s on the firing probability of the post-synaptic cell; conversely, one could also infer, from cross-correlograms, the shapes of underlying p.s.p.s. Although the relation between p.s.p.s and correlograms has been theoretically analysed, few empirical comparisons have been made. Moore *et al.* (1970) have argued that the shape of the primary correlogram peak produced by an e.p.s.p. should resemble the wave form of the underlying e.p.s.p., because 'to a first approximation the instantaneous firing probability of a neuron is inversely related to the instantaneous distance between the membrane potential and threshold'. Indeed, they found that e.p.s.p.s in *Aplysia* neurones produced primary correlogram peaks that broadly matched the e.p.s.p.s. Similarly, in motoneurones of the crayfish claw, the correlogram peaks resemble the e.p.s.p.s, although not all e.p.s.p.s generate correlogram peaks (Lindsley & Gerstein, 1979).

In contrast to these results, theoretical analyses of neural models have led to the conclusion that e.p.s.p.s would produce correlogram peaks that resemble their temporal derivative. This relation reflects the fact that the membrane trajectory of the post-synaptic cell would typically cross threshold for firing during the rise of the e.p.s.p. For a neurone model that reached a threshold firing level by integrating e.p.s.p.s, and reset the membrane trajectory after firing, Knox (1974) found that the resulting correlograms resembled the derivatives of a variety of e.p.s.p. shapes. Further tests of this model confirmed that 'the primary synaptic effect appears in the cross-correlation function as a distorted version of the derivative of the p.s.p.' (Knox & Poppele, 1977). Assuming such a relation, others have used the integral of post-stimulus firing probability of human motor units to infer the shape of underlying p.s.p.s in motoneurones (Ashby & Labelle, 1977; Ashby & Zilm, 1978, 1982*b*; Homma & Nakajima, 1979).

Still a third possibility was suggested by Kirkwood & Sears (1978) in their analysis of the synaptic events underlying the average common excitation potential in inspiratory motoneurones. They proposed that the primary correlogram peak could be the sum of two linear terms: one proportional to the e.p.s.p., the second proportional to its temporal derivative. The two proportionality constants could be chosen to provide good theoretical matches to observed average common excitation potentials (Kirkwood & Sears, 1978) and short-term synchronization of intercostal motoneurones (Sears & Stagg, 1976). Compiling cross-correlograms between intercostal muscle afferents and ventral root efferents during respiration, Kirkwood & Sears (1982) found correlogram peaks whose shapes could plausibly resemble the sum of such terms, given the shapes of single-fibre e.p.s.p.s documented in separate experiments.

The present study was designed to compare directly the time course of p.s.p.s and the corresponding correlogram features in mammalian motoneurones. Intracellular micro-electrodes in cat lumbar motoneurones were used to record p.s.p.s and to produce repetitive firing by current injection. E.p.s.p.s and i.p.s.p.s of varying amplitudes were evoked by electrical stimulation of peripheral nerve filaments; first with the motoneurone quiescent, to document the average p.s.p. shape, and then with the motoneurone firing repetitively, to document the cross-correlogram between

stimulus and spike trains. Direct comparisons of their time course in the same motoneurons suggest that in most cases, simple e.p.s.p.s produce correlogram peaks that resemble their temporal derivatives, although the onset of the correlogram peak is delayed by about 0.5 msec. Complex e.p.s.p.s and large i.p.s.p.s, however, produced correlogram features that deviated significantly from their temporal derivatives.

METHODS

The results presented were obtained from lumbar motoneurons recorded in eleven cats; six cats were anaesthetized with α -chloralose (40–50 mg/kg *i.v.*) and five with sodium pentobarbitone (Nembutal, 30–40 mg/kg *i.p.* supplemented with 5 mg/kg as needed). All animals were paralysed with gallamine triethiodide (Flaxedil), and artificially respired. Bilateral pneumothorax was always performed to reduce respiratory movements. End-tidal CO_2 was measured on a Beckmann medical gas analyser and kept around 4%. Arterial blood pressure was monitored continuously and was always above 80 mmHg. Motoneurons in the L7 and L6 lumbar segments were identified by antidromic responses to ventral root stimulation and by the types of synaptic potentials evoked from identified peripheral nerves. The following nerves were routinely prepared for electrical stimulation: posterior biceps-semitendinosus, semimembranosus-anterior biceps, peroneal, quadriceps, flexor digitorum longus, gastrocnemius, and plantaris. In five cats, the nerves to the gastrocnemius muscle were left intact and the distal end of the muscle was attached to a stretcher, to provide a source of synaptic noise. In these experiments, the gastrocnemius nerve was split into small filaments, which were separately placed on stimulating electrodes.

Motoneurons were recorded with glass pipettes filled with 2 M-K citrate. The tips of the micro-electrodes were broken back to a diameter of 1.5–2.0 μm and had a resistance when measured in saline of 2–5 M Ω . After a motoneuron was impaled, the p.s.p.s evoked from the nerve filaments were identified. P.s.p.s and correlograms were obtained while the peripheral nerves were stimulated at rates of 2–30/sec. In initial experiments, stimuli were delivered randomly, but direct comparisons with regular stimulus trains indicated that the same primary correlogram features were obtained with regular and random stimulation. The p.s.p. wave form was first averaged while the motoneuron was quiescent; then the motoneuron was made to fire repetitively by intracellular injection of depolarizing currents, typically 10–50 nA (Fig. 1). Repetitive firing was continued long enough (90–200 sec) to generate a clear post-stimulus time histogram of motoneuron firing. Firing rate was adjusted to be different from the stimulus rate, to prevent entrainment by stimulus trains. The mean firing rate of motoneurons during computation of correlograms was 16.1 ± 4.1 impulses/sec. (s.d.) This firing rate was primarily determined by the injected current, rather than the nerve stimulation, as indicated by two factors. The mean firing rate calculated as the total number of spikes divided by the duration of the computation period differed negligibly from the pre-p.s.p. base-line firing rate in the cross-correlograms. The base-line rates were slightly lower than the net firing rate, by about 0.6 impulses/sec for small (< 1.0 mV) evoked e.p.s.p.s and by 0.9 impulses/sec for larger e.p.s.p.s; neither deviation was statistically significant. Moreover, the number of spikes in the correlogram peaks was a small fraction of the total number of spikes, even with the largest e.p.s.p.s. For e.p.s.p.s larger than 1 mV, this fraction was 0.01–0.06 ($n = 8$) for stimulus frequencies of 2–3/sec and 0.11–0.20 for frequencies of 10–12/sec. Lower fractions were obtained for smaller e.p.s.p.s. Thus, the motoneurons were clearly firing rhythmically, independently of the applied p.s.p.s (cf. Fig. 1).

An analogue tape recorder with a band width of 0–10 kHz was used to record (1) voltage pulses marking the stimuli, (2) intracellular recordings of the motoneuron membrane potential, (3) cord dorsum potentials at the dorsal root entry, and (4) pulses triggered from motoneuron action potentials during repetitive firing. E.p.s.p. amplitudes were usually calibrated by 1 mV calibration pulses. In addition to on-line averaging with a CAT Nemetron averager, tape-recorded records were used for subsequent off-line analysis. A Nicolet averager was used to compile average p.s.p.s and corresponding cross-correlograms of stimulus trains and motoneuron firing (Fig. 1). These cross-correlograms were post-stimulus averages of 0.2 msec pulses triggered from the start of the motoneuron action potentials. The Nicolet averager was also used to calculate the temporal derivative of the averaged p.s.p.s, and the integral of the cross-correlograms.

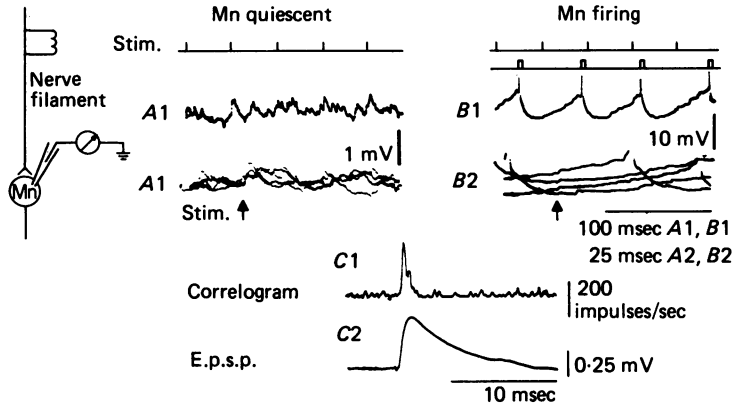


Fig. 1. Schematic diagram of experimental conditions. Peripheral nerve filaments were stimulated (stim.) electrically to evoke p.s.p.s in lumbar motoneurones (mn). Intracellular records were obtained with motoneurone quiescent (*A1*, *A2*) and firing repetitively (*B1*, *B2*). Intracellular records are shown at the same sweep speed as the stimulus train in *A1* and *B1*, and are synchronized with successive stimuli in *A2* and *B2*, to show evoked e.p.s.p.s at arrows. The average e.p.s.p. (*C2*) was computed by summing records, as in *A2*. The cross-correlogram (*C1*) was computed by compiling the post-stimulus time histogram of pulses (0.2 msec duration) triggered from motoneurone action potentials.

RESULTS

Amplitude of cross-correlogram peaks produced by e.p.s.p.s

The relation between simple e.p.s.p.s and their corresponding correlograms was examined for a group of thirty-eight e.p.s.p.s, ranging in size from 0.15 to 3.1 mV (mean height = 0.75 ± 0.67 mV (s.d.)). Fig. 2 shows examples of four representative e.p.s.p.s with different height and rise times, and their associated cross-correlograms. As illustrated, the larger e.p.s.p.s generally produced higher and sharper correlogram peaks, while smaller e.p.s.p.s produced correlogram peaks that were broader and noisier (Fig. 2*A*). For a given size of e.p.s.p., those with slower rise times generally produced wider correlogram peaks.

The relative amplitude of the correlogram peak to base-line firing rate was calculated by dividing the maximum firing rate in the peak by the average firing rate preceding the e.p.s.p. This amplitude ratio is plotted against e.p.s.p. amplitude in Fig. 3*A*. The Figure shows that the height of the correlogram peak increased with the e.p.s.p. size; the regression line fitted to these points has a slope of 23.7/mV. The values plotted in Fig. 3*A* represent the maximum firing rate in the correlogram peak; another measure of increased firing might be the *mean* firing rate throughout the peak – from its onset to its return to base-line rates. This mean relative increase in firing during the entire correlogram peak, when plotted against e.p.s.p. amplitude, resembles the plot shown in Fig. 3*A*, except that values of the mean rates in the peak are generally about one-third of the maximal rates.

The height of the correlogram peak was also related to the e.p.s.p. derivative as illustrated in Fig. 3*B*, which plots the relative amplitude of the correlogram peak as a function of the maximum rate of rise of the e.p.s.p. The e.p.s.p.s with faster rise

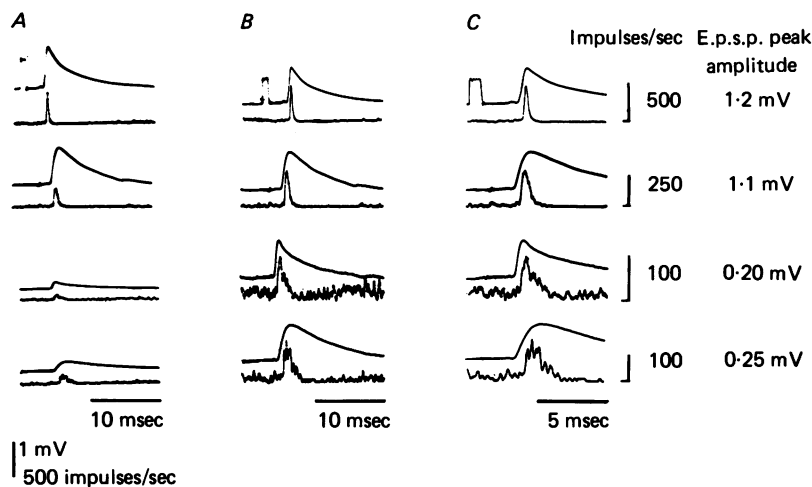


Fig. 2. Comparison of four representative e.p.s.p.s and resulting cross-correlograms. From top to bottom, records illustrate larger and smaller e.p.s.p.s with fast and slow rise. *A*, e.p.s.p.s and cross-correlograms at same vertical gain, to compare amplitudes. *B*, normalized records at slow sweep, to compare the time course of e.p.s.p.s with the primary peak and trough of correlograms. *C*, fast sweep to show the relative timing of correlogram peak and e.p.s.p. Base of correlogram calibration bar indicates zero level. Stimulation rates, from top to bottom, were 11, 10, 30 and 25/sec.

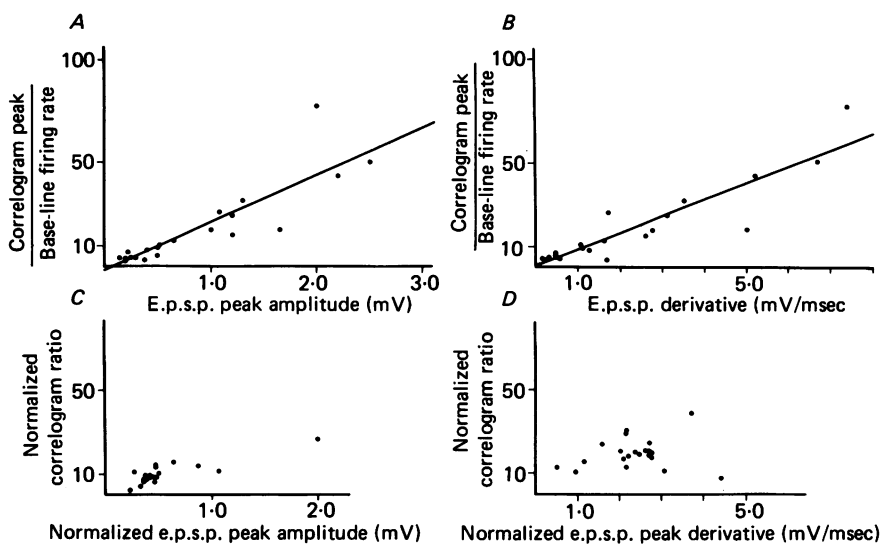


Fig. 3. Height of correlogram peak as a function of e.p.s.p. parameters. *A*, relative amplitude of correlogram peak to base-line firing rate as a function of e.p.s.p. amplitude. Ordinate plots maximum height of correlogram peak divided by pre-e.p.s.p. base-line firing rate. *B*, relative amplitude of correlogram peak to base line as a function of maximum positive slope of e.p.s.p. (mV/msec). The derivative of the e.p.s.p. was computed electronically and its peak value used for the abscissa. Straight lines represent regression lines. Since *A* and *B* indicate that the correlogram peak increased both with larger e.p.s.p. and with larger e.p.s.p. derivatives, values were separately normalized to same derivative (*C*) and to same e.p.s.p. amplitude (*D*). Normalized plots suggest a somewhat better relation to e.p.s.p. amplitude.

times generated proportionately larger correlogram peaks. The slope of the regression line is $8.1/\text{mV} \cdot \text{msec}$.

Since the larger e.p.s.p.s generally had faster rising slopes, the two plots in Fig. 3*A*, *B* do not indicate whether the amplitude of the correlogram peak ultimately depends more on the e.p.s.p. amplitude or derivative. Comparison of e.p.s.p.s that have similar amplitudes and different derivatives (or vice versa) was not possible in enough cases to resolve the issue (but cf. top e.p.s.p.s in Fig. 2*A*). To determine whether the correlogram peak depended linearly only on e.p.s.p. amplitude or only on e.p.s.p. derivative, we used separate normalization procedures to test each hypothesis. The correlograms and e.p.s.p.s were thus normalized to an e.p.s.p. peak derivative of $1 \text{ mV}/\text{msec}$ by dividing each peak amplitude by the corresponding e.p.s.p. derivative (Fig. 3*C*). In a similar manner, correlogram peaks and e.p.s.p. derivatives were normalized to an e.p.s.p. peak amplitude of 1 mV (Fig. 3*D*). This normalization procedure gives a significant increase in correlogram peak with increased e.p.s.p. peak amplitude (slope of regression line: $11.3/\text{mV}$, $P < 0.01$) and no change with increased peak derivative (slope $1.4/\text{mV} \cdot \text{msec}$, $P < 0.05$), suggesting that the amplitude of the correlogram peak may depend more on the e.p.s.p. peak amplitude than on the e.p.s.p. peak derivative. However, these experimental data are clearly too few and scattered to allow any final conclusion.

Width of correlogram peaks

The duration of the correlogram peak was typically briefer than that of the e.p.s.p., and was more closely related to the duration of the e.p.s.p. rise. This is shown in Fig. 4*A*, which plots the duration of the correlogram peak, measured from onset to end, against the time-to-peak of the e.p.s.p. The e.p.s.p.s with longer rise times produced wider correlogram peaks. However, the size of the e.p.s.p. had some effect on this relation. For large e.p.s.p.s, with peak amplitudes greater than 1 mV , the points are distributed about the line indicating equality between correlogram duration and e.p.s.p. time-to-peak; for smaller e.p.s.p.s, the correlogram duration was typically longer than the e.p.s.p. time-to-peak. This is further illustrated in Fig. 4*B*, where the ratio of the correlogram peak duration to the e.p.s.p. time-to-peak is plotted against the peak amplitude of the e.p.s.p.s. The mean value of this ratio was 1.45 ± 0.42 s.d. for all e.p.s.p.s less than 1 mV ($n = 18$), compared with a mean of 1.05 ± 0.34 for e.p.s.p.s greater than 1 mV ($n = 18$). Thus, the correlogram peaks of larger e.p.s.p.s often matched the duration of their rise times, while correlograms of smaller e.p.s.p.s exceeded the rise times ($P < 0.05$).

The width of the correlogram peak was also compared with the duration of the entire e.p.s.p. The average half-width of the correlogram peaks ($0.65 \pm 0.28 \text{ msec}$, $n = 38$) was much shorter than the mean half-width of these e.p.s.p.s ($4.3 \pm 1.5 \text{ msec}$). The individual ratios of correlogram half-widths to e.p.s.p. half-widths are plotted in Fig. 4*C* as a function of e.p.s.p. amplitude. The average ratio was 0.20 ± 0.06 for e.p.s.p.s below 1 mV , and 0.13 ± 0.06 for larger e.p.s.p.s, with appreciable variance in individual values. Thus, the larger e.p.s.p.s generated narrower correlogram peaks relative to the e.p.s.p. width ($P < 0.05$).

The mean half-width of the correlogram peaks ($0.65 \pm 0.28 \text{ msec}$) was similar to that of the e.p.s.p. derivative ($0.55 \pm 0.33 \text{ msec}$). The individual ratios of correlogram

half-widths to derivative half-widths are plotted in Fig. 4D against e.p.s.p. amplitude. Small e.p.s.p.s showed a considerable range of values, and their correlogram peaks were often wider than their derivative curves; for the larger e.p.s.p.s, the correlogram peaks and derivatives were often similar in width. These data suggest that the increase in firing probability correlated with e.p.s.p.s does not last throughout the e.p.s.p., but rather approximates the rise time of the e.p.s.p.

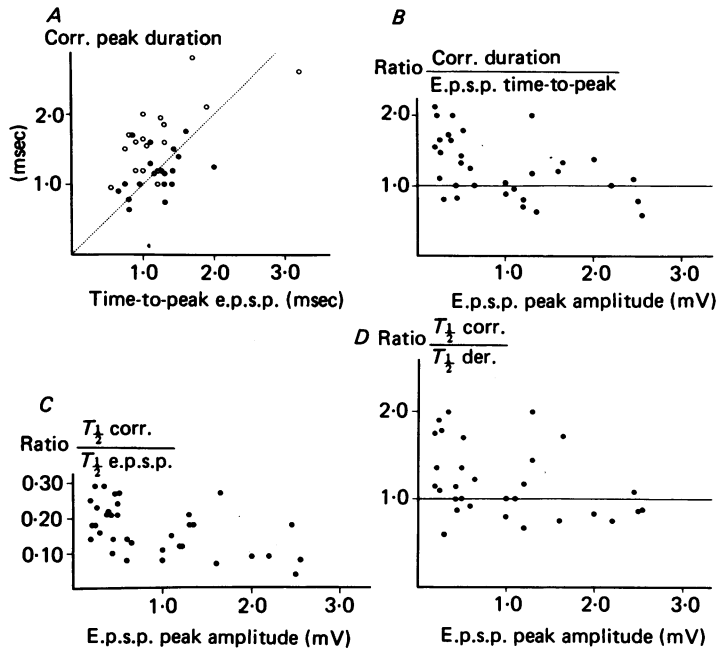


Fig. 4. Width of correlogram peak as function of e.p.s.p. parameters. *A*, duration of correlogram (corr.) peak (time from onset to time of first return to base-line value) plotted against time-to-peak of e.p.s.p. (from onset). Points indicate separately the e.p.s.p.s that were larger (●) and smaller (○) than 1 mV. *B*, ratio of correlogram duration to e.p.s.p. time-to-peak, plotted as a function of e.p.s.p. maximum amplitude. *C*, ratio of correlogram half-width ($T_{1/2}$ corr.) to e.p.s.p. half-width ($T_{1/2}$ e.p.s.p.), plotted as a function of e.p.s.p. amplitude. *D*, ratio of correlogram half-width to half-width of e.p.s.p. derivative ($T_{1/2}$ der.), plotted as a function of e.p.s.p. amplitude.

Relation between shape of correlogram peak and e.p.s.p. derivative

To determine how closely the shape of the correlogram peak matched the e.p.s.p. derivative, we computed the temporal derivatives of the e.p.s.p.s and compared them with the correlogram peaks and their subsequent troughs. We tested this relation further by computing the integral of the correlogram (relative to base line) and comparing it with the e.p.s.p. Representative results are shown in Fig. 5 for four e.p.s.p.s of different sizes and slopes. The upper records (*A1–D1*) show in successive lines the e.p.s.p. and its temporal derivative, and the cross-correlogram with its integral. To facilitate comparison of wave forms, we equated the amplitudes of corresponding records. The middle records show corresponding traces superimposed, to illustrate the temporal delay in the correlogram records. The correlogram peaks

began to rise after the onset of the e.p.s.p., with an average delay of 0.48 ± 0.19 msec ($n = 38$). These delays tended to be shorter for the larger e.p.s.p.s; most delays were $300\text{--}400$ μsec for e.p.s.p.s larger than 1 mV, and $400\text{--}650$ μsec for smaller e.p.s.p.s. Fast-rising e.p.s.p.s had a weak tendency to be associated with shorter delays, but the data points were too scattered to allow any conclusion. Except for this temporal delay, the shapes of corresponding records in Fig. 5 were similar.

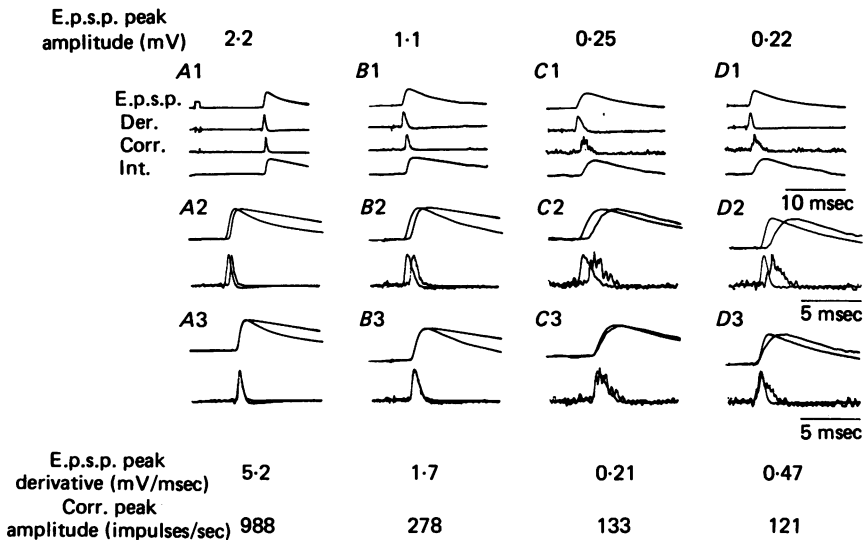


Fig. 5. Comparison of time course of cross-correlogram features with e.p.s.p. derivatives, and of correlogram integrals with e.p.s.p.s. Four representative sizes of e.p.s.p. shown in A–D. Top (A1–D1) shows separate records of the e.p.s.p. and its temporal derivate (der.), the cross-correlogram (corr.) and its integral (int.). To obtain a flat base line for the integral, the pre-e.p.s.p. base-line firing rate in the correlogram was taken as zero. The height of the derivative and integral were normalized to match the height of correlogram peak and e.p.s.p., respectively. Middle records (A2–D2) show corresponding curves superimposed to illustrate the temporal delay in the correlogram records. Bottom records (A3–D3) align onset of corresponding curves to compare their time course.

To compare their time course in more detail, the bottom set of records (A3–D3) shows the records shifted in time so that their onsets are superimposed. The time course of the correlogram peak matches the positive component of the e.p.s.p. derivative rather well, especially for the larger e.p.s.p.s (A3, B3). For the smaller e.p.s.p.s the correlogram peaks were often wider than the e.p.s.p. derivative (D3). Some mismatch also is evident during the falling phase of the larger e.p.s.p., where the e.p.s.p. derivative becomes more negative than the correlogram trough. For the two larger e.p.s.p.s (A3, B3), the e.p.s.p. derivative shows a negative overshoot while the correlogram trough is limited to zero firing rate. The same relation is also evident in comparing the e.p.s.p. and the correlogram integral: their rising edges match well in A3 and B3, but the e.p.s.p. drops off faster than the integral of the correlogram. In contrast, for many of the smaller e.p.s.p.s the correlogram trough did not reach the limit of zero firing rate. As illustrated in Fig. 5 (see also Fig. 6), the correlogram trough often dropped below base-line rates by an amount roughly comparable to the

negative component of the derivative. This agreement between the correlogram trough and negative slope is also shown by the fact that the decay of the integrated correlogram approximates the decay of the small e.p.s.p.s (*C3, D3*).

Small e.p.s.p.s in synaptic noise

The effects of small e.p.s.p.s superimposed with synaptic noise of comparable amplitudes are particularly relevant to understanding the consequences of unitary e.p.s.p.s for cross-correlograms. Results for seven such cases are illustrated in Fig. 6. As shown in the upper records, the synaptic noise is large enough to obscure the evoked e.p.s.p.s. The averaged e.p.s.p.s and their correlogram peaks are shown with the e.p.s.p. derivative. As described above for small e.p.s.p.s, the correlogram peaks are similar to or slightly wider than the e.p.s.p. derivative peak, but are briefer than

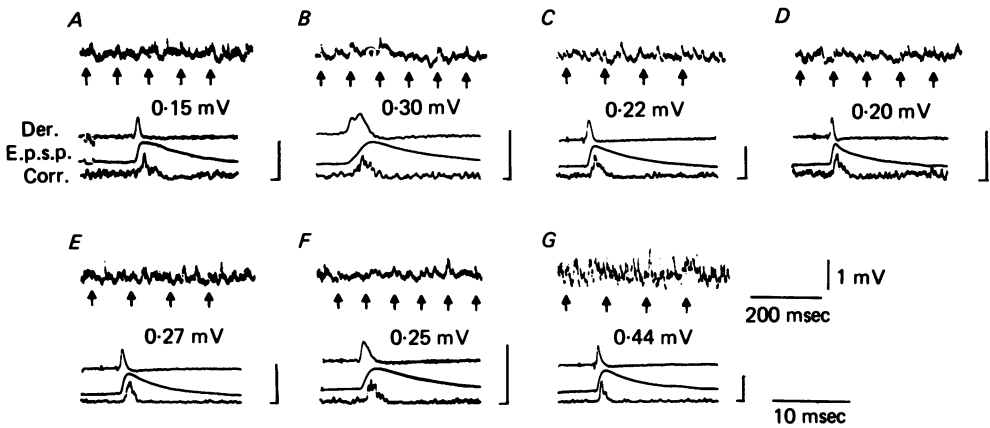


Fig. 6. Correlograms of small e.p.s.p.s in synaptic noise of comparable amplitude. Top lines illustrate intracellular records, with occurrence of evoked e.p.s.p.s indicated by arrows. The average of each e.p.s.p. is shown, with its computed temporal derivative (der.) above and its corresponding cross-correlogram (corr.) below. The amplitude of the derivative was normalized to match the amplitude of the correlogram peak. Correlogram calibration bars: *A-D*, 200 impulses/sec; *E-G*, 400 impulses/sec.

the e.p.s.p. itself. Examination of the records indicates that each correlogram peak is followed by a trough, in which firing rate drops below base line, during the time that the e.p.s.p. is decaying.

It has been suggested that the correlogram produced by a unitary e.p.s.p. could be approximated by a linear combination of the e.p.s.p. and its derivative (Kirkwood & Sears, 1978, 1982; Kirkwood, 1979). To test whether the wider correlograms associated with small e.p.s.p.s could be fit better by such a combination, a term proportional to the e.p.s.p. was added to the derivative. The results did not provide a better match for all correlogram features, for reasons illustrated in Fig. 7. The correlogram peak of this cell was wider than the e.p.s.p. derivative (*A*). Adding an e.p.s.p. component (*B*, lower-most record) to the derivative yields a wave form whose peak is wider than the derivative (*B*, upper-most records) and overlaps better with the correlogram peak (*C*). However, this combination is now mismatched with the trough, since the e.p.s.p. term has cancelled the negative component of the derivative. This mismatch is clearly evident in the integrals of the records (*D*); the integrated

correlogram decays (like the e.p.s.p.) due to its trough, whereas the integral of the combined e.p.s.p.-derivative wave form increases with time (*D*, upper record). Reducing the e.p.s.p. component will reduce the mismatch in the trough, but will correspondingly increase the discrepancy of the peaks. Similar results were obtained with other e.p.s.p.-derivative combinations.

For small e.p.s.p.s, the correlogram peaks, which were wider than the derivative, typically rose more slowly than the derivative. As illustrated for the cell in Fig. 7, the rising phase of these correlograms sometimes showed a better fit with the rise of the e.p.s.p. (*E*, *F*) than its derivative (*A*). To test quantitatively whether the

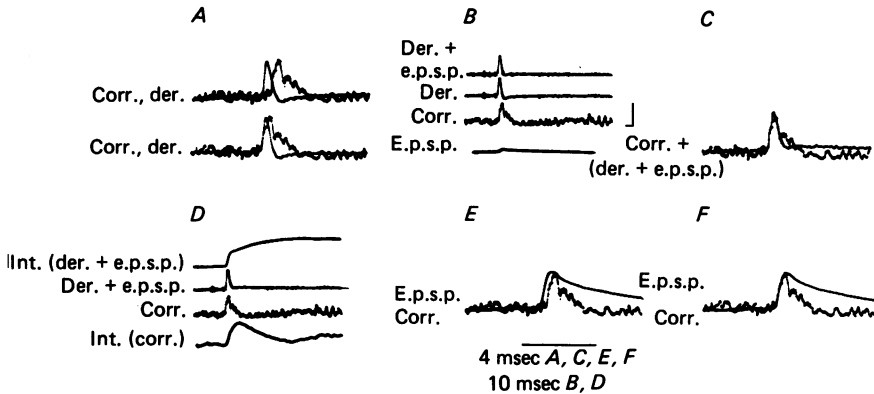


Fig. 7. Matches between correlogram and wave forms proportional to e.p.s.p. (*F*), e.p.s.p. derivative (*A*), and the sum of e.p.s.p. and derivative (*C*). *A*, superposition of correlogram and e.p.s.p. derivative without temporal shift (top) and after alignment of onsets (bottom). *B*, separate display of wave forms proportional to e.p.s.p., its derivative (der.), and their sum (der. + e.p.s.p.). *C*, best superposition of correlogram and summed wave form. The summed wave form provides a better match than the derivative for the correlogram peak, but a prolonged mismatch for the trough. *D*, integral of summed wave form int.(der. + e.p.s.p.) at the top shows a prolonged rise; by comparison, integral of correlogram int.(corr.) at the bottom decays due to trough. *E*, *F*, superposition of correlogram with e.p.s.p. to illustrate match between rising phase; records are shown without temporal shift in *E*, and with onsets aligned in *F*. The e.p.s.p. amplitude was 200 μ V. Correlogram bar: 100 impulses/sec.

correlogram rise might be related more closely to the rise of the e.p.s.p. than the derivative, we compared the differentiated records as shown in Fig. 8. The e.p.s.p. and its derivative, the correlogram and its integral (*A1*, *B1*) were electronically smoothed and normalized to the same peak amplitude (*A2*, *B2*); these records were then differentiated (*A3*, *B3*) to obtain a clear measure of their rising phase. For the large e.p.s.p. (*A*), the differentiated correlogram resembles the differentiated derivative, as expected from the good match between correlogram and e.p.s.p. derivative. In contrast, for the smaller e.p.s.p. (*B*), the positive component of the differentiated correlogram resembles the differentiated e.p.s.p. better than the differentiated derivative, indicating that the rising phase of the correlogram resembles the e.p.s.p. more closely than its derivative. Using the peaks of the differentiated records as a basis for comparison, Fig. 8*C*, *D* shows individual values for e.p.s.p.s of various sizes. The ratio of the peaks of the differentiated correlogram and derivative varies around unity for all e.p.s.p.s (*C*), indicating a good agreement between the

rising phase of the correlogram and the e.p.s.p. derivative for all but the smallest e.p.s.p.s. In contrast, the ratio of the peaks of the differentiated correlogram and the e.p.s.p. was larger than one for all e.p.s.p.s (*D*), indicating that the correlograms rose more steeply than the e.p.s.p. These records indicate that for most e.p.s.p.s the rising phase of the correlogram fits the e.p.s.p. derivative better than the e.p.s.p. However, for an appreciable fraction of the small e.p.s.p.s, the correlogram is only slightly steeper than the rising phase of the e.p.s.p.

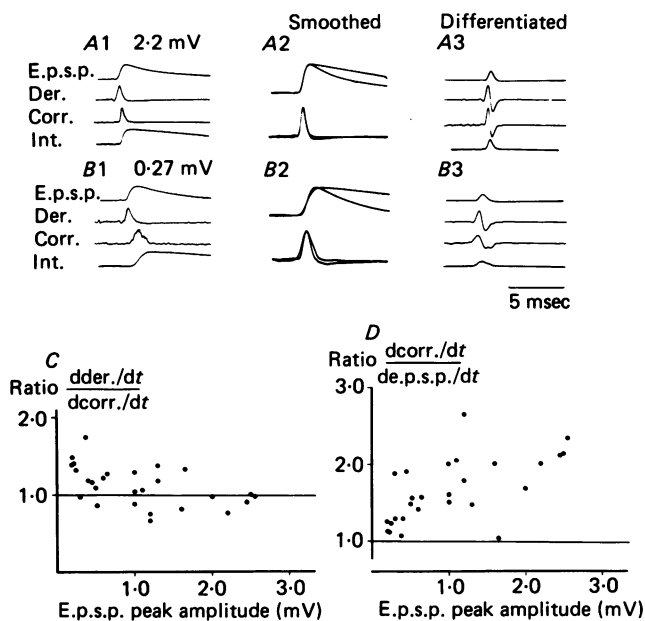


Fig. 8. Comparison between rising phase of correlogram peaks and rise of e.p.s.p.s. Illustrative records for large (*A1–A3*) and small (*B1–B3*) e.p.s.p.s, showing separate normalized wave forms (*A1, B1*), smoothed superimposed records (*A2, B2*) and differentiated records (*A3, B3*). *C*, ratio of maxima of differentiated e.p.s.p. derivative and correlogram peak, plotted as a function of e.p.s.p. amplitude. *D*, ratio of maxima of differentiated correlogram peak and e.p.s.p. as a function of e.p.s.p. amplitude. (See text.)

Complex e.p.s.p.s

Compound p.s.p.s, composed of e.p.s.p.s with more complex wave forms, often produced cross-correlograms that deviated from the e.p.s.p. derivative. For example, the e.p.s.p. in Fig. 9*A* exhibited two components in the rising phase, producing two corresponding peaks in its temporal derivative; however, these derivative peaks are not reflected in the cross-correlogram, which is unimodal. Moreover, the falling phase of the e.p.s.p. has both fast and slow components evident in its derivative but not in the correlogram trough, which is limited at zero.

A second example (Fig. 9*B*) is an e.p.s.p. whose rising phase has two slopes, a rapid initial rise followed by a slower rise to its summit. Again, these two slope components are not accurately reflected in the correlogram peak, which is broader than the large derivative peak and does not show the subsequent slow component.

Double e.p.s.p.s were sometimes evoked, as shown in Fig. 9*C* and *D*, to test for

linear summation of the correlogram peaks. The derivative of the two equally large e.p.s.p.s in Fig. 9C shows two peaks of equal amplitude; in contrast, the corresponding correlogram shows unequal peaks, indicating that the second e.p.s.p. produced a much smaller increment in firing than the initial e.p.s.p. Thus, while the e.p.s.p.s and their derivatives exhibit linear summation, the correlogram peaks do not. Fig. 9D shows the summation of two smaller e.p.s.p.s. In this case, the resultant cross-correlogram seems to be a better approximation to the temporal derivative; the relative amplitudes of the correlogram peaks are comparable to those of the

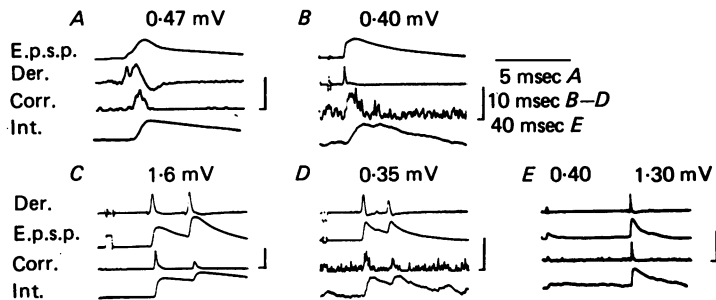


Fig. 9. Correlograms produced by complex e.p.s.p.s. Records illustrate averaged e.p.s.p. and its temporal derivative (der.), the associated correlogram (corr.) and its integral (int.). *A, B*, compound e.p.s.p. with two components on rising edge. *C*, summation of two large e.p.s.p.s of same size. *D*, summation of smaller e.p.s.p. with larger e.p.s.p. *E*, small and large e.p.s.p.s separated by long interval. Values of e.p.s.p. peaks indicate scale. Correlogram bars: *A, C, E*, 500 impulses/sec; *B*, 100 impulses/sec; *D*, 200 impulses/sec.

derivative peaks. The fact that Fig. 9C showed greater reduction in the second correlogram peak than in Fig. 9D is probably related to the e.p.s.p. size: the first e.p.s.p. is five times larger in Fig. 9C.

Fig. 9E compares the effects of a small and a large e.p.s.p. separated by 40 msec. The amplitude of the correlogram peak produced by the larger e.p.s.p. was proportionately larger than that produced by the small e.p.s.p. The integrated correlogram also showed peaks whose relative amplitudes were similar to those of the e.p.s.p.s. In four cells examined with two e.p.s.p.s, the amplitude ratios of the e.p.s.p.s were 4.4, 4.1, 3.1 and 2.3 (the smaller e.p.s.p.s had amplitudes of 0.5–1.0 mV); the corresponding integrated correlogram peaks had ratios of 3.9, 3.6, 4.2 and 3.1. Thus, the relative amplitudes of the e.p.s.p.s were reflected in the relative heights of the integrated correlograms.

Correlograms produced by i.p.s.p.s

The effects of compound i.p.s.p.s on the cross-correlogram are illustrated by representative examples in Fig. 10. I.p.s.p.s, evoked by stimulating nerves of antagonist muscles, produced correlograms whose primary feature was a trough followed by a shallow peak. The time course of this sequence was distinctly different from the derivative of the i.p.s.p. As indicated in Fig. 10 (*A1, A2* and *B1*), the motoneurone firing probability dropped to zero through the peak of the i.p.s.p.; this was followed by a rebound increase in firing beginning during the decay of the i.p.s.p.

Since the correlogram trough is limited at zero rate, its time course cannot be a linear function of either the i.p.s.p. or its derivative. The duration of the correlogram trough clearly exceeds that of the i.p.s.p. derivative, yet is briefer than the duration of the i.p.s.p. itself. In these records, the onset of the trough follows the onset of the i.p.s.p. by 0.2 msec.

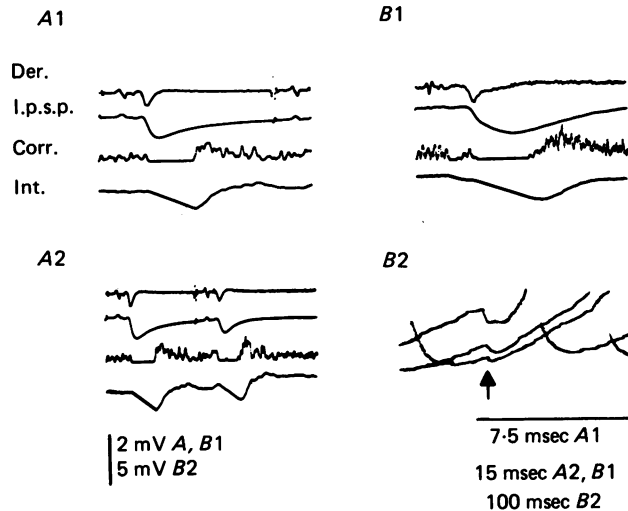


Fig. 10. Effects of i.p.s.p.s on motoneurone firing probability. Records of i.p.s.p. and its temporal derivative (der.) are shown with associated cross-correlogram (corr.) and its integral (int.). *A1, B1*, two different i.p.s.p.s with fast and slow rise. *A2*, the same i.p.s.p. as in *A1* at slower sweep showing the response to a second, smaller i.p.s.p. evoked 9 msec later. *B2*, motoneurone membrane trajectories during repetitive firing, with evoked i.p.s.p.s aligned at arrows.

Fig. 10 (*B2*) illustrates the membrane trajectories of an active motoneurone with the evoked i.p.s.p.s aligned in the middle of the sweep (arrow). As indicated, the i.p.s.p.s that occurred when the membrane potential was close to threshold retarded the occurrence of a motoneurone action potential for the duration of the i.p.s.p. peak.

The amplitudes of these compound i.p.s.p.s exceeded 1 mV with the motoneurone at rest. As shown in Fig. 10 (*B2*), the size of the i.p.s.p.s increased substantially as the motoneurone membrane potential approached threshold. The non-linear relation between the shapes of the i.p.s.p.s and their correlogram features may well be a consequence of their size; they were sufficiently large to arrest motoneurone firing during their peaks.

DISCUSSION

The p.s.p.-correlogram transform

In an active neurone, p.s.p.s produce correlated changes in firing probability that appear as primary peaks and troughs in the cross-correlogram between the source of the synaptic input and the neurone's action potentials (Bryant *et al.* 1973; Kirkwood, 1979; Knox, 1974; Moore *et al.* 1966, 1970; Perkel, Gerstein & Moore, 1967). The possible relations between the shapes of the p.s.p. and the resultant correlogram features have been analysed theoretically, but empirical data have

remained relatively indirect. Three different linear transforms have been proposed on theoretical grounds. If firing probability were inversely related to instantaneous distance to a voltage threshold, the correlogram would be expected to resemble the p.s.p. itself (Moore *et al.* 1970). On the other hand, if threshold is typically crossed during the rising (depolarizing) phase of the p.s.p., the correlogram should resemble the temporal derivative of the p.s.p. (Knox, 1974). Evidence from respiratory motoneurons led Kirkwood & Sears (1978, 1982) to propose a third possibility: that the correlogram resembles a linear sum of the p.s.p. and its derivative. In this latter view, a p.s.p. with time course $e(\tau)$ would be transformed to the correlogram $f(\tau)$ by the linear 'operator':

$$f(\tau) = a e(\tau) + b \frac{de(\tau)}{d\tau},$$

where the parameters a and b would be different constants for different cells (Kirkwood, 1979), and τ is time from the source of the p.s.p.

To test these different hypotheses experimentally, we compared the slopes of p.s.p.s in lumbar motoneurons with the time course of the primary correlogram features that they produced during repetitive firing. The closest approximation to a linear transform appeared with smooth aggregate e.p.s.p.s; such e.p.s.p.s generated a correlogram peak and trough sequence that often closely resembled the e.p.s.p. derivative. However, characteristic deviations from a good match seemed to be associated with smaller e.p.s.p.s, increased levels of synaptic noise, and complex wave forms.

Another non-linear feature was a temporal delay between the onset of the e.p.s.p. and the onset of the correlogram peak. This delay, averaging almost 0.5 msec, was not simply a consequence of triggering the correlogram pulses late on the rising edge of the action potential, since the trigger threshold was carefully set at the onset of the initial segment spike. This delay probably reflects some minimal utilization time required for the membrane currents to initiate the action potential at the axon hillock. Larger e.p.s.p.s would be expected to have shorter utilization times, and in our data the correlograms of larger e.p.s.p.s did have shorter delays. This delay may also include conduction time of the p.s.p. from the site of p.s.p. recording to the site of spike initiation, and conduction time of the action potential to the recording site. The comparison between p.s.p. and correlogram shapes was made after they were temporally shifted for optimal overlap.

The range of e.p.s.p.s studied allowed the amplitude of the correlogram peak to be related to e.p.s.p. parameters. As indicated in Fig. 3, the relative amplitude of the correlogram peak above base-line rates was an increasing function of both the amplitude and the rising slope of the e.p.s.p.s. In the present data, amplitude and slope of e.p.s.p.s also covaried with each other, so normalization procedures were used to separate these variables. The results suggest that the height of these correlogram peaks varied more fundamentally with e.p.s.p. amplitude than with rising slope, but this trend is based on too small a sample to warrant any definite conclusions. Recent observations with stretch-evoked e.p.s.p.s indicate that small e.p.s.p.s with similar amplitude but differing slopes produced correlogram peaks whose size increased with the e.p.s.p. derivative (B. Gustafsson & D. McCrea, unpublished observations).

The half-widths of the correlogram peaks produced by aggregate e.p.s.p.s approximated the half-widths of the e.p.s.p. derivatives much better than the widths of the e.p.s.p.s themselves (Fig. 4). Kirkwood & Sears (1982) found similar relations for unitary e.p.s.p.s generated in intercostal motoneurons by single muscle spindle afferents: their cross-correlograms between afferent spikes and ventral root spikes had peaks with half-widths (mean 0.99 msec) that tended to be closer to the rise times (mean 0.77 msec) than the half-widths (4.7 msec) of unitary e.p.s.p.s obtained in separate experiments by spike-triggered averaging. Our mean values for evoked e.p.s.p.s in lumbar motoneurons are in good agreement; however, direct comparisons of individual correlogram peaks with their corresponding e.p.s.p.s suggest appreciable scatter about these means (Fig. 4). Moreover, as e.p.s.p.s became smaller and more comparable in size to membrane voltage fluctuations, our correlogram peaks became wider than the derivative half-width, consistent with Kirkwood & Sears' observation for unitary e.p.s.p.s.

In direct comparisons, the time course of the correlogram features generally resembled the time course of the e.p.s.p. derivative, although characteristic differences between large and small e.p.s.p.s (relative to 1 mV) were apparent. The correlogram *peaks* matched the positive phase of the e.p.s.p. derivative better for large e.p.s.p.s than for smaller e.p.s.p.s, which generated peaks wider than the e.p.s.p. derivative (Figs. 5 and 6). On the other hand, the subsequent correlogram *trough*, in which firing fell below base line, approximated the negative component of the e.p.s.p. derivative better for small e.p.s.p.s, mainly because the trough was often limited at zero for large e.p.s.p.s. Most of the smaller e.p.s.p.s produced correlograms with a smooth trough, whose integral matched the fall of the e.p.s.p. These results are explicable in terms of the probabilities of crossing threshold during these e.p.s.p.s, as discussed below.

Our attempt to fit the correlogram features by adding terms proportional to the e.p.s.p. and its derivative produced mixed success (Fig. 7). Although the amplitudes of two such terms could sometimes be adjusted to better match the wider correlogram peaks of small e.p.s.p.s in synaptic noise, this combination then failed to match the subsequent trough. The term proportional to the e.p.s.p. generally lasted so long that it eliminated or reversed the trough when added with sufficient amplitude to widen the peak. In contrast, the single-unit cross-correlogram peaks of Kirkwood & Sears (1982) were not followed by a trough; instead some of their peaks had a shallow 'tail', in qualitative agreement with their predictions. Several differences in their experimental conditions could explain these different results. Their single-fibre e.p.s.p.s were typically much smaller than our composite e.p.s.p.s; the upper end of their range (200 μ V) corresponds to the lower end of ours. Secondly, their intercostal motoneurons were activated by synaptic input, generating synaptic noise several times greater than we produced, even with muscle stretch (Fig. 6). Moreover, during the inspiratory phase, when their correlograms were compiled, their e.p.s.p.s commonly exhibited prolonged tails, with multiple 'humps' of depolarization. For reasons discussed below, these factors could well explain correlogram peaks with tails instead of troughs.

Our results with large e.p.s.p.s generally confirm the theoretical predictions of Knox (1974) and Knox & Poppele (1977), based on a model of e.p.s.p.s superimposed on a membrane trajectory that approached a constant voltage threshold. Our

observations also lend empirical support to the use of the integral of the post-stimulus firing probability of human motor units to estimate the initial time course of the underlying aggregate e.p.s.p.s. In active soleus motor units of human subjects, Ashby & Labelle (1977) documented post-stimulus effects produced by group I volleys in extensor muscle nerves; the duration of the primary correlogram peak (3.6 msec) was taken as a measure of the rise time of the underlying e.p.s.p. Their correlogram peaks were wider than ours, probably due to larger afferent volleys and to greater temporal dispersion of conduction in afferent and efferent pathways. Similar results were obtained in tibialis anterior motor units (Ashby & Zilm, 1978, 1982*b*). Using triangular muscle stretches, Homma & Nakajima (1979) measured post-stimulus responses of gastrocnemius motor units in humans; integrating the primary correlogram peak evoked by stretching the soleus, they estimated the rise of the compound e.p.s.p. to be 4.7 msec. These experimenters also used inhibitory synaptic input from antagonist muscles to produce primary correlogram troughs; the observed decreases in motor unit firing lasted considerably longer than the correlogram peaks associated with excitatory input from synergists (Ashby & Labelle, 1977; Homma & Nakajima, 1979). These results are consistent with our findings that aggregate i.p.s.p.s generated correlogram troughs wider than the peaks produced by e.p.s.p.s of comparable duration. The fact that the correlogram trough produced by large i.p.s.p.s was not simply related to the shape of the i.p.s.p. or its derivative (Fig. 10) would suggest that the integral of the cross-correlogram produced by aggregate i.p.s.p.s cannot be used to reconstruct the shape of the underlying i.p.s.p.

Threshold crossings of a motoneurone model

The observed relations between primary cross-correlogram features and underlying p.s.p.s can be understood qualitatively in terms of a model in which the p.s.p.s are superimposed on a membrane trajectory approaching threshold (Knox, 1974; Ashby & Zilm, 1982*a*). This type of model, shown in Fig. 11, yields a close relation between the correlogram peak and the e.p.s.p. derivative. The membrane trajectory of a repetitively firing motoneurone is shown in Fig. 11*A* with two e.p.s.p.s occurring during an interspike interval. The second e.p.s.p. occurs at a time when the membrane trajectory is sufficiently close to threshold that the e.p.s.p. would initiate an action potential; in effect, this e.p.s.p. advances the occurrence of the second action potential to its rising phase. Fig. 11*B* illustrates these events from the point of view of a time axis aligned with the onset of the e.p.s.p.s. The stimuli that initiate the e.p.s.p.s occur at the origin of this time axis, which is also the abscissa of the cross-correlogram in *C*. To simplify analysis without losing generality, we can first represent the e.p.s.p., $e(\tau)$, as rising and falling linearly, with a peak height, h . The difference between the motoneurone membrane trajectory and voltage threshold preceding an action potential is designated as $v(\tau)$ and is represented as a linear function in Fig. 11*B*. In the absence of any e.p.s.p., the average firing probability of the motoneurone would be a constant, f_0 , as a function of time, τ , after the 'stimulus'; i.e. the correlogram would be flat (Fig. 11*C*). Evoking an e.p.s.p. regularly at time τ_0 would change the post-stimulus firing probability as shown by the heavy line in Fig. 11*C*. This change can be calculated by considering those action potentials whose occurrence is advanced by the e.p.s.p. For example, the action potential that would have occurred at time

τ_3 in the absence of an e.p.s.p. is now initiated at time τ_1 since the voltage difference between the membrane trajectory and the threshold preceding the action potential, $v(\tau)$, is exceeded by the e.p.s.p. at τ_1 . Similarly, all action potentials that would have occurred in the interval τ_0 - τ_4 now occur in the interval τ_0 - τ_2 . This model, therefore,

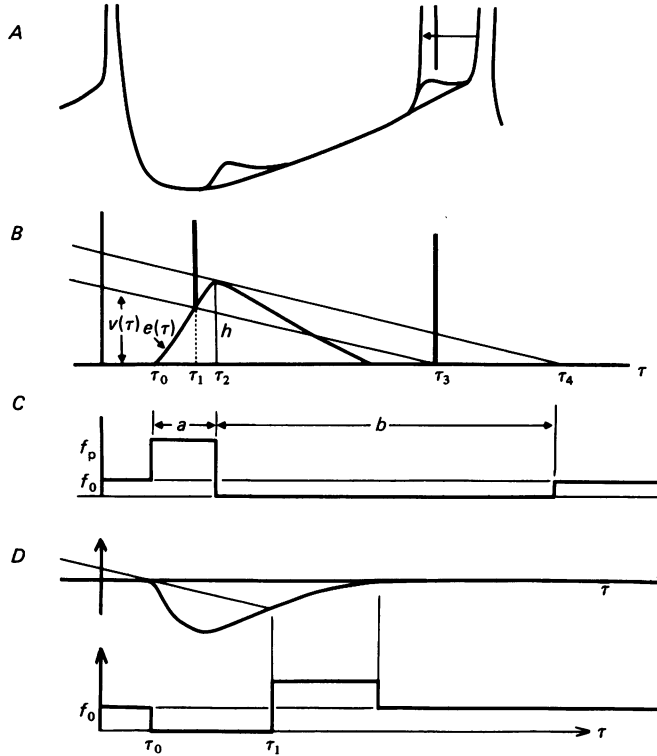


Fig. 11. A model predicting the effects of post-synaptic potentials on motoneurone firing probability. *A*, motoneurone membrane trajectory during interspike interval showing two superimposed e.p.s.p.s. $v(\tau)$ is the difference between voltage threshold and membrane potential. The second e.p.s.p. advances an action potential. *B*, voltage events on time axis aligned with stimuli evoking e.p.s.p. Simplified e.p.s.p. $e(\tau)$ rises linearly from onset at τ_0 to peak h at τ_2 and decays linearly. The difference between membrane potential and threshold ($v(\tau)$), decreasing linearly with time, is shown preceding an action potential that would have occurred at τ_3 , but is initiated by e.p.s.p. at τ_1 . τ_4 is the time of the last action potential that would be advanced by the e.p.s.p. (to τ_2). *C*, firing probability of motoneurone as function of time τ after stimulus event. Without any e.p.s.p., the firing probability is constant, f_0 . An e.p.s.p. advances action potentials, increasing firing probability between τ_0 and τ_2 and decreasing it between τ_2 and τ_4 . f_p is value of peak of correlogram. *D*, effects of i.p.s.p.s on cross-correlogram. Action potentials occurring between onset of i.p.s.p. (τ_0) and point of intersection with indicated trajectory of $v(\tau)$ would be delayed to times after τ_1 .

predicts that the duration of the correlogram peak equals the rise time of the e.p.s.p., in agreement with our results for large e.p.s.p.s (Fig. 4 *B*). The model further predicts that the height of the correlogram peak above base line ($f_p - f_0$) is proportional to the e.p.s.p. slope, as follows: Let N = number of action potentials advanced by the e.p.s.p., $a = \tau_2 - \tau_0$ = duration of correlogram peak, $b = \tau_4 - \tau_2$ = duration of

correlogram trough, $de/d\tau = h/a =$ rising slope of e.p.s.p., $\dot{v} = dv/d\tau = h/b =$ rate of closure between membrane potential and threshold, then

$$N = f_0(a+b) = f_p a.$$

Therefore

$$\begin{aligned} f_p &= f_0(1 + [b/a]) \\ &= f_0 \left(1 + \frac{1}{\dot{v}} \frac{de}{d\tau} \right). \end{aligned}$$

Thus, during its rise, the triangular e.p.s.p. would produce an increment in firing above the base line of

$$f_p - f_0 = \left(\frac{f_0}{\dot{v}} \right) \frac{de}{d\tau},$$

which is proportional to the first derivative of the e.p.s.p.

Although this calculation assumed a linear rise and fall for the e.p.s.p., the same analysis would apply to time-dependent e.p.s.p.s, $e(\tau)$, which can be piecewise linearly approximated (Fig. 12). For the smaller time-dependent e.p.s.p., illustrated in Fig. 12A, the number of spikes advanced into an interval $\Delta\tau_1$ following τ_1 from interval $\Delta\tau_3$ following τ_3 would be given by

$$dn(\tau_1) = f(\tau_1) \Delta\tau_1 = f_0 \Delta\tau_3.$$

For the affected spikes, the intervals $\Delta\tau_1$ and $\Delta\tau_3$ have the relation

$$\Delta\tau_3 = \Delta\tau_1 + \frac{\Delta e}{\dot{v}} = \Delta\tau_1 \left(1 + \frac{1}{\dot{v}} \frac{de(\tau)}{d\tau} \right).$$

Thus, the firing rate $f(\tau)$ in the correlogram peak is:

$$f(\tau) = f_0 + \frac{f_0}{\dot{v}} \frac{de(\tau)}{d\tau}.$$

This expression is valid so long as $de/d\tau \geq -\dot{v}$, which is equivalent to the condition that $f(\tau)$ must be ≥ 0 . If the e.p.s.p. decay rate exceeds \dot{v} (as illustrated for the large e.p.s.p. in Fig. 12), the corresponding firing rate would drop to zero, since intercepts are precluded over an interval whose duration is determined by the 'shadow' cast by the e.p.s.p. peak intercepting the trajectories, $v(\tau)$. These correlogram functions are plotted in Fig. 12B for two time-dependent e.p.s.p.s, which differ in magnitude and in their corresponding temporal derivative.

Thus, the noiseless-threshold-crossing model predicts many of the empirically observed relations. The shape of the correlogram *peak* generated by the model matches the time course of the positive derivative of the e.p.s.p. Such a match was observed for many of the larger e.p.s.p.s, for which the assumption of a smooth approach to threshold is valid (Fig. 5). Moreover, if the e.p.s.p. decays more slowly than \dot{v} , the above equation would also hold for the falling phase of the e.p.s.p. In such a case, illustrated for the small e.p.s.p. in Fig. 12, the negative values of the e.p.s.p. derivative would yield a proportional drop in firing rate below the base line, generating the correlogram *trough*. Empirically, many of the small e.p.s.p.s did show a good match between the correlogram trough and the negative e.p.s.p. derivative (Figs. 5 and 6). For large e.p.s.p.s whose decay rate exceeds \dot{v} , the absence of intercepts

in the shadow cast by the peak yields a zero firing rate. Empirically, large e.p.s.p.s commonly generated correlogram troughs with zero firing rate (Fig. 5).

Thus, assuming a smooth motoneurone trajectory approach to threshold, the model predicts that the ratio of the correlogram peak height above base line to base line ($[f_p - f_0]/f_0$) would be proportional to the e.p.s.p. derivative; the proportionality constant is the reciprocal of \dot{v} , the rate of closure between membrane potential and threshold. The term \dot{v} depends on the time course of the voltage threshold as well as on the membrane potential. If the voltage threshold is constant during the interspike interval (Calvin & Stevens, 1968; Kernell, 1972), \dot{v} equals the absolute slope of the membrane potential trajectory. But evidence from statistical analysis of interspike intervals (Calvin & Stevens, 1968) and direct threshold testing (Calvin, 1974) suggests that in some cases the voltage threshold may be rising towards the end of the interval; in this case, \dot{v} would be less than the membrane potential slope. An estimate of this term from the line fitted to the points in Fig. 3B would be $\dot{v} = 0.13$ mV/msec, which is compatible with published records (Schwindt & Calvin, 1972; Baldissera & Gustafsson, 1974; Calvin, 1974).

The effect of e.p.s.p.s evoked by repetitive activation of afferent fibres on motoneurone firing rate is usually considered to be equivalent to the mean depolarization (or mean current) produced by the e.p.s.p.s, i.e. equivalent to intracellularly injected constant current (Granit, Kernell & Lamarre, 1966). Although the present experimental and theoretical data stress the importance of the e.p.s.p. derivative in determining the shape of the correlogram peak, the data are not at variance with the importance of the e.p.s.p. voltage itself in governing the net change in firing rate. In fact, the threshold-crossing model predicts that the mean increase in firing rate produced by an 'unshadowed' e.p.s.p. (whose decay is less than \dot{v}) is proportional to the mean e.p.s.p. amplitude, averaged over time. As seen in Fig. 12, the spikes advanced to τ_1 from τ_3 by the smaller e.p.s.p. are associated with a decrease in interspike interval of

$$\Delta T(\tau_1) = \tau_1 - \tau_3 = -\frac{e(\tau_1)}{\dot{v}}.$$

The average decrease in all interspike intervals produced by such e.p.s.p.s, if e.p.s.p.s occur at a rate of $f_e = 1/T_e$, is

$$\begin{aligned} \overline{\Delta T} &= \frac{1}{T_e} \int_0^{T_e} \Delta T(\tau) f(\tau) d\tau \\ &= \frac{1}{T_e} \int_0^{T_e} \left(-\frac{e(\tau)}{\dot{v}} \right) \left(1 + \frac{1}{\dot{v}} \frac{de}{d\tau} \right) d\tau \\ &= -\frac{\bar{e}}{\dot{v}}, \end{aligned}$$

where \bar{e} is the average depolarization produced by the (unshadowed) e.p.s.p.s. The corresponding mean increase in motoneurone firing rate would then be:

$$\overline{\Delta f} = -\frac{\overline{\Delta T}}{T_e^2} = \frac{f_e^2 \bar{e}}{\dot{v}}.$$

This relation holds only for 'unshadowed' e.p.s.p.s, whose decay rates remain less than \dot{v} . For larger e.p.s.p.s, with faster decay rate, a part of the falling phase will

be 'shadowed' by the e.p.s.p. peak, precluding interception with any trajectories. For such an e.p.s.p., the mean spike advancement will be related not to its mean depolarization, but rather to the mean voltage of an 'equivalent unshadowed e.p.s.p.' whose decay is equal to $v(\tau)$ in the shadowed interval (Fig. 12). The mean increase in motoneurone firing frequency produced by the large e.p.s.p. would then be greater than its mean depolarization level, by an amount proportional to the difference between the areas of the real e.p.s.p. and its 'equivalent unshadowed e.p.s.p.' (shaded area in Fig. 12). Thus, the noiseless model predicts that e.p.s.p.s would produce a net increase in firing rate as large as that produced by their average depolarization (unshadowed e.p.s.p.s) or larger (shadowed e.p.s.p.s).

Qualitative explanation of non-linear transforms

Synaptic noise. The above model has assumed that the motoneurone membrane potential approaches threshold smoothly and linearly. Normally, other p.s.p.s would be superimposed on the membrane trajectory, producing voltage fluctuations comparable in size to the correlated e.p.s.p. The effect of these fluctuations could be qualitatively estimated by considering the illustrated membrane trajectory, $v(\tau)$, preceding an action potential to represent the *mean* of a set of trajectories, each deviating from the mean by superimposed fluctuations. As a consequence, some smooth trajectories that would have missed the e.p.s.p. (those producing action potentials occurring at $\tau > \tau_4$) now have a chance of intercepting the e.p.s.p. This would enhance the probability of firing about the peak of the e.p.s.p., including times past the peak. The effect of such random fluctuations on the membrane trajectory would be to broaden the correlogram peak, making it wider than the e.p.s.p. derivative; such broadening was, in fact, observed for small e.p.s.p.s accompanied by substantial synaptic noise (Fig. 5) (Kirkwood & Sears, 1982).

The noiseless-motoneurone model, with smooth membrane trajectories, predicts a correlogram peak proportional to the e.p.s.p. derivative; the effect of superimposed synaptic noise can be considered to add a second term representing the additional probability of threshold crossing. The exact shape of this additional term would depend on the frequency spectrum and amplitude distribution of the synaptic noise, as well as on the shape of the e.p.s.p. Kirkwood & Sears (1978, 1982) suggested this additional term might be proportional to the e.p.s.p. itself. In our records, the correlogram peaks produced by small e.p.s.p.s in synaptic noise required an additional term somewhat shorter than the e.p.s.p.; such a term should contribute preferentially near the peak of the e.p.s.p. and decrease faster than the e.p.s.p. to avoid cancelling the correlogram trough.

Generation of such a non-linear term could be qualitatively explained by the motoneurone model in terms of the threshold crossings produced by the synaptic noise. Considering the trajectories diagrammed in Fig. 11B, it is clear that a major contribution to this additional term derives from mean approach trajectories $v(\tau)$ above the e.p.s.p., which now could intercept the e.p.s.p. by virtue of the statistical fluctuations about their mean. Two factors would tend to favour interceptions around the peak of the e.p.s.p., *versus* crossings during the tail of the e.p.s.p. Since the noise amplitude distribution drops off as a function of distance from the mean trajectory, the peak of the e.p.s.p. has a greater net chance of being intercepted by higher trajectories than the base of the e.p.s.p. The faster the decay rate of the e.p.s.p.

compared with the rate of closure, $dv/d\tau$, the more the peak will be preferentially intercepted (cf. Fig. 12). The second factor favouring earlier threshold crossing is that a given trajectory can intercept the e.p.s.p. only once; after crossing threshold and initiating a spike, the trajectory is eliminated from further interaction. Since interception late in the e.p.s.p. is contingent on the absence of any preceding threshold crossing, the probability of the first crossing occurring later in the e.p.s.p., decreases with time. Consequently, the triggering of spikes during the initial part of

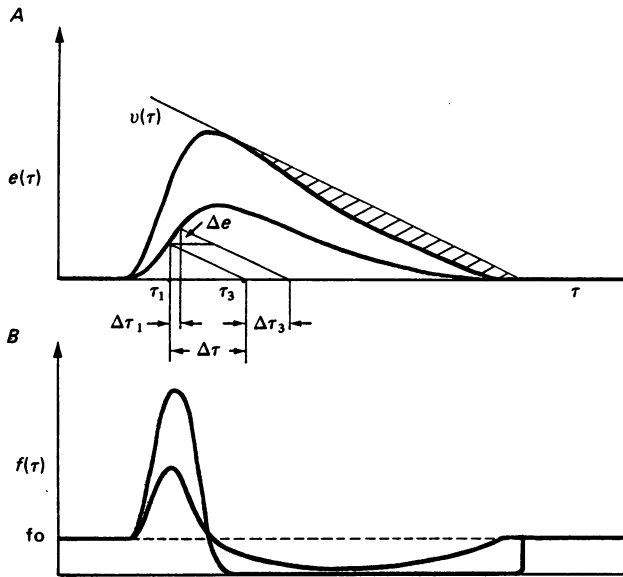


Fig. 12. Transform between time-dependent e.p.s.p., $e(\tau)$, and corresponding correlogram e.p.s.p., $f(\tau)$, predicted by a motoneurone model with smooth membrane trajectories to threshold. The difference between membrane potential and threshold, $v(\tau)$, is assumed to decrease at a constant rate, \dot{v} . The large e.p.s.p. differs from the small e.p.s.p. in amplitude, such that its decay rate ($de/d\tau$) exceeds \dot{v} . In the shaded region, the decay phase of the large e.p.s.p. is 'shadowed' by its peak, precluding threshold crossings, and producing a correlogram firing probability of zero.

the e.p.s.p. is favoured. The higher the frequency spectrum of the noise fluctuations relative to the e.p.s.p., the more will this factor favour early crossings. This factor also helps explain the non-linear summation of correlogram peaks produced by a pair of large e.p.s.p.s (Fig. 9C); when the e.p.s.p. interval is shorter than the interspike interval, the number of trajectories available for interaction with the second e.p.s.p. is reduced by their intersection with the first.

I.p.s.p.s. The simple voltage-threshold model above also provides a qualitative explanation for the correlogram features associated with aggregate i.p.s.p.s. The fact that the primary correlogram trough exceeds the duration of the i.p.s.p. derivative would be a consequence of the fact that the i.p.s.p. rising slope exceeds $dv/d\tau$. As shown in Fig. 11D, the end of the correlogram trough occurs when $v(\tau)$ intercepts the falling phase of the i.p.s.p. The subsequent compensatory correlogram peak arises from the delayed action potentials. Although the noiseless model predicts a trough

that drops to zero firing rate, the existence of appreciable synaptic noise would tend to smooth out these correlogram features. More recent results indicate that small i.p.s.p.s in synaptic noise can generate correlogram features better resembling the i.p.s.p. derivative (B. Gustafsson & D. McCrea, unpublished observations).

In our analysis, the shapes of the correlogram features have been compared to the time course of p.s.p.s measured with the motoneurone at rest. As is evident from Fig. 11 *A*, the more relevant factor for predicting the correlogram from the voltage model is the shape and size of the p.s.p. near threshold (Knox & Poppele, 1977). With regard to e.p.s.p.s, the experimental evidence of Edwards, Redman & Walmsley (1976) suggests that the shape of unitary Ia e.p.s.p.s changes minimally over several millivolts of depolarization; the major change is an occasional increase in the falling slope of the e.p.s.p. During rhythmic firing at low frequencies, the conductance near the end of the interspike interval should approach that at rest (Baldissera & Gustafsson, 1974), suggesting that at the low firing rates used (10–20 impulses/sec) the e.p.s.p.s near threshold should resemble those measured at rest. In contrast to the e.p.s.p.s, the i.p.s.p.s had appreciably greater amplitude near threshold than at rest (Fig. 10). This would increase the duration of the resulting correlogram trough over those predicted on the basis of i.p.s.p.s measured at rest, and further exaggerate the non-linear relation between aggregate i.p.s.p.s and their correlograms.

The degree to which the present results with motoneurons will hold for other types of neurones remains to be demonstrated. The above model, involving a nearly linear approach to voltage threshold for spike initiation and interspike intervals exceeding the duration of p.s.p.s, is characteristic of rhythmically firing motoneurons, and explains qualitatively most of the observed relations between p.s.p. shape and correlogram features. To the extent that other neurones exhibit similar firing mechanisms, one might anticipate similar relations. However, in neurones capable of firing repetitively during the time course of a single p.s.p., the correlogram features may prove to reflect more the shape of the p.s.p. itself.

We thank Drs Elzbieta Jankowska and Holger Wigström for helpful discussions, Ms Rauni Larsson for technical assistance during experiments, Mr Thomas Palm for help with photography, and Ms Kate Schmitt for editorial assistance. This work was supported by the Swedish Medical Research Council, a Josiah Macy Faculty Scholar Award (E.F.), and NIH grants NS12542 (E.F.) and RR00166 (Regional Primate Research Center at the University of Washington).

REFERENCES

- ASHBY, P. & LABELLE, K. (1977). Effects of extensor and flexor group I afferent volleys on the excitability of individual soleus motoneurons in man. *J. Neurol. Neurosurg. Psychiat.* **40**, 910–919.
- ASHBY, P. & ZILM, D. (1978). Synaptic connections to individual tibialis anterior motoneurons in man. *J. Neurol. Neurosurg. Psychiat.* **41**, 684–689.
- ASHBY, P. & ZILM, D. (1982*a*). Relationship between EPSP shape and cross-correlation profile explored by computer simulation for studies on human motoneurons. *Exp. Brain Res.* **47**, 33–40.
- ASHBY, P. & ZILM, D. (1982*b*). Characteristics of postsynaptic potentials produced in single human motoneurons by homonymous group 1 volleys. *Exp. Brain Res.* **47**, 41–48.
- BALDISSERA, F. & GUSTAFSSON, B. (1974). Firing behavior of a neurone model based on the afterhyperpolarization conductance time course and algebraic summation. Adaptation and steady state firing. *Acta physiol. scand.* **92**, 27–47.
- BRYANT, H. L., MARCOS, A. R. & SEGUNDO, J. P. (1973). Correlation of neuronal spike discharges produced by monosynaptic connections and by common inputs. *J. Neurophysiol.* **36**, 205–255.

- CALVIN, W. H. (1974). Three modes of repetitive firing and the role of threshold time course between spikes. *Brain Res.* **69**, 341–346.
- CALVIN, W. H. & STEVENS, C. F. (1968). Synaptic noise and other sources of randomness in motoneuron interspike intervals. *J. Neurophysiol.* **31**, 574–587.
- EDWARDS, F. R., REDMAN, S. J. & WALMSLEY, B. (1976). The effect of polarizing currents on unitary Ia excitatory post-synaptic potentials evoked in spinal motoneurons. *J. Physiol.* **259**, 705–723.
- GRANIT, R., KERNELL, D. & LAMARRE, Y. (1966). Algebraic summation in synaptic activation of motoneurons firing within the 'primary range' to injected currents. *J. Physiol.* **187**, 379–399.
- HOMMA, S. & NAKAJIMA, Y. (1979). Input–output relationship in spinal motoneurons in the stretch reflex. *Prog. Brain Res.* **50**, 37–43.
- KERNELL, D. (1972). The early phase of adaptation in repetitive impulse discharges of cat spinal motoneurons. *Brain Res.* **41**, 184–186.
- KIRKWOOD, P. A. (1979). On the use and interpretation of cross-correlation measurements in the mammalian central nervous system. *J. Neurosci. Meth.* **1**, 107–132.
- KIRKWOOD, P. A. & SEARS, T. A. (1978). The synaptic connexions to intercostal motoneurons as revealed by the average common excitation potential. *J. Physiol.* **275**, 103–134.
- KIRKWOOD, P. A. & SEARS, T. A. (1982). The effects of single afferent impulses on the probability of firing of external intercostal motoneurons in the cat. *J. Physiol.* **322**, 315–336.
- KNOX, C. K. (1974). Cross-correlation functions for a neuronal model. *Biophys. J.* **14**, 567–582.
- KNOX, C. K. & POPPELE, R. E. (1977). Correlation analysis of stimulus-evoked changes in excitability of spontaneously firing neurons. *J. Neurophysiol.* **40**, 616–625.
- LINDSLEY, B. G. & GERSTEIN, G. L. (1979). Interactions among an ensemble of chordotonal organ receptors and motor neurons of the crayfish claw. *J. Neurophysiol.* **42**, 383–399.
- MOORE, G. P., PERKEL, D. H. & SEGUNDO, J. P. (1966). Statistical analysis and functional interpretation of neuronal spike data. *A. Rev. Physiol.* **28**, 493–522.
- MOORE, G. P., SEGUNDO, J. P., PERKEL, D. H. & LEVITAN, H. (1970). Statistical signs of synaptic interaction in neurons. *Biophys. J.* **10**, 876–900.
- PERKEL, D. H., GERSTEIN, G. L. & MOORE, G. P. (1967). Neuronal spike trains and stochastic point processes. II. Simultaneous spike trains. *Biophys. J.* **7**, 419–440.
- SCHWINDT, P. C. & CALVIN, W. H. (1972). Membrane potential trajectories between spikes underlying motoneuron firing rates. *J. Neurophysiol.* **35**, 311–325.
- SEARS, T. A. & STAGG, D. (1976). Short-term synchronization of intercostal motoneurone activity. *J. Physiol.* **263**, 357–381.